JOURNAL OF SANDWICH STRUCTURES & MATERIALS

Standard Article

The role of sodium silicate treated randomly distributed jute fiber core on the mechanical, thermal and fire behavior of novel sandwich structures

Journal of Sandwich Structures & Materials
2025, Vol. 0(0) 1–24

DOI: 10.1177/10996362251357088
journals.sagepub.com/home/jsm
Sage

Ahsanul Islam, Chinmoy Biswas, Md Arifuzzaman, Raju Ahammad, Shahinur Hasnat Rahat and Md Shariful Islam

Abstract

In this work lightweight and fire-resistant sandwich structures were fabricated and their mechanical, thermal, and fire behavior were investigated. The non-woven mat consisting of jute and polyester fibers at a ratio of 60:40 was used to manufacture Hybrid fiber reinforced Sodium silicate Composites (HSC) to be used as the core of the sandwich structure. The concentration of sodium silicate solution was varied (i.e., 80%, 90%, and 100%) to manufacture HSCs. The woven Jute fiber mat reinforced Epoxy Composites (JEC) were prepared using hand layup followed by light compression method to be used as the skins of the sandwich structures. The tensile and flexural test results revealed that HSC with 100% sodium silicate concentration showed increased strength and modulus. The thermal conductivity was not significantly affected by the sodium silicate solution concentration to prepare HSC and the thermal conductivity of the sandwiches are significantly lower than many existing jute-fiber based composites. However, the fire spread, and damage propagation during fire exposure test were significantly affected by the sodium silicate solution concentration. Sandwich with 100% sodium silicate solution concentration is found to have minimum damage due to fire exposure for 30 minutes. These findings provide a comprehensive understanding of the fabrication processes and

Department of Mechanical Engineering, Khulna University of Engineering & Technology, Khulna, Bangladesh

Corresponding author:
Md Arifuzzaman, Department of Mechanical Engineering, Khulna University of Engineering & Technology, Khulna 9203, Bangladesh.
Email: arif48@me.kuet.ac.bd

design of the sandwich structures using HSC and JEC for applications where high strength, insulation, and fire resistance are required together.

Keywords
Non-woven hybrid fiber mat, sodium silicate solution, mechanical properties, thermal exposure, fire exposure

Introduction

Lightweight composite laminates have various applications including building, ships and aircrafts[1] because of their multifunctionality. These laminates or sandwich structures must provide sufficient strength, durability, protection against corrosive environment, thermal insulation, etc. However, along with every technological development come difficulties, especially when it comes to waste management. The disposal of composite materials is a major issue since many synthetic composites are not biodegradable and require a long time to break down, which contributes to long-term pollution of the environment. The usage of these materials might have a detrimental effect on marine ecosystems and water quality.[2,3] Because of that, there is a growing tendency to reconsider the usage of natural fiber-based composites since they provide a more environmentally friendly substitute for synthetic materials. The attractive features of these fibers are ecological advantages and availability. These fibers are environmentally friendly, biodegradable, renewable and provide the facility to be used as a green source of reinforcing materials. The low density, high specific strength, and modulus properties of these fibers showed the potential to be used in fiber reinforced composites for load-bearing applications with partial replacement of synthetic fibers.[4,5] Nowadays fiber-reinforced composites are being developed and redesigned sustainably and responsibly to improve and adapt traditional products and introduce new products. Natural fibers such as jute, flax, coir, sisal, etc. Are widely used as reinforcing fibers in thermoset and thermoplastic matrices. Among these fibers, jute is a commercially available and inexpensive source of lignocellulosic fiber. The typical chemical composition of this fiber is cellulose (51%–84%), hemicellulose (12%–20%), lignin (5%–13%), pectin (0.2%), and wax (0.5%).[6] Cellulose is considered the major framework component of the fiber structure. It provides strength, stiffness, and structural stability of the fiber.[7]

Although jute fiber based composites have some impactful advantages, they possess significant drawbacks such as high moisture absorption, lower mechanical properties, flammable, etc..[8,9] Researchers are trying to overcome these limitations by undertaking various measures. For instance, the alkali treatment of fibers using 5% NaOH solution showed significant improvements in mechanical properties of jute fiber reinforced composites.[10] Chandramohan et al.[3] investigated mechanical and thermal properties by hybridizing jute fiber with aloe vera, using epoxy resin, hardener, and adhesives. Three types of samples were prepared: aloe vera, jute, and jute-aloe vera hybrid composites. The study revealed an increase in flexural strength, tensile strength, and water absorption

percentage in the case of the jute-aloe vera hybrid composite. However, no significant variation was observed in impact testing among the three specimens. Overall, the hybridization of jute and aloe vera led to improved mechanical and thermal properties of the composites. Bisaria et al.[11] discussed the mechanical properties according to the change in the fiber length. They found that the composite of 15 mm length occupied the maximum tensile and flexural properties. Wang et al.[12] described that in terms of stiffness and cost, natural fiber is comparatively better than glass fiber. Natural fiber has a low density which leads to better comparison for specific properties. Moreover, it was proposed that further improvement of moisture resistance and fire retardant will be possible to extend its application range. Rajole et al.[13] investigated the ballistic energy absorption of natural fiber composites, focusing on jute-epoxy (JE) and jute-epoxy-rubber (JRE) sandwich composites. Results indicated that thickness significantly impacted energy absorption in JE composite plates. Furthermore, JRE sandwiches exhibit approximately 71% greater energy absorption than JE plates. Elbadry et al.[14] combined recycled needle-punched jute fiber mats as core reinforcement and recycled jute fabric cloths as skin layers in unsaturated polyester matrix composites using a modified hand lay-up technique. Results showed improved tensile and flexural properties with increasing fiber content and the addition of jute fabric skins. Fajrin et al.[15] investigated the flexural behavior of hybrid sandwich panels incorporating jute fiber composite (JFC) and hemp fiber composite (HFC) as intermediate layers, compared to conventional sandwich panels without an intermediate layer. Aluminum sheets served as skins, and expanded polystyrene (EPS) was used for the core. Static flexural tests revealed significantly enhanced load-carrying capacity in hybrid panels, with JFC increasing it by 29.60% and HFC by 93.46%. Hybrid panels exhibited greater toughness and sustained larger strains before ultimate loads. Failure modes varied, with indentation and core shear in conventional panels, and core shear and delamination in hybrids. Intermediate layers improved deformation capability and load-bearing capacity.

Manfredi et. al.[16] investigated the thermal behavior and fire resistance of jute-reinforced composites with vinylester and resol matrices, enhanced by the addition of organically modified clay. Thermogravimetric analysis showed that clay significantly improved the thermal resistance of the composites. Fire resistance was evaluated through cone calorimetry, which demonstrated a reduction in the peak heat release rate with clay addition, though it did not significantly affect ignition time or total heat release. Palsule et al. focused[17] on the thermal stability of jute fiber reinforced high-density polyethylene (JF/CF-HDPE) composites, developed using the Palsule process without any compatibilizer or fiber treatment. The degradation of the composites initiated at temperatures between those of the fiber and matrix. Mainly, the maximum degradation temperature of all composite compositions was higher than that of the matrix and increased with higher jute fiber content. For the 10/90, 20/80, and 30/70 JF/CF-HDPE composites, the highest rate of degradation occurred at 483°C, 485°C, and 488°C, respectively, with residual masses of 4.3%, 5.8%, and 7% at 550°C. Boopalan et. al.[18] investigated the thermal properties of jute and banana fiber reinforced epoxy hybrid composites with varying fiber ratios (100/0, 75/25, 50/50, 25/75, and 0/100). Results showed that mixing up to 50%

banana fiber into the jute/epoxy composites enhanced their thermal properties. The hybrid composites indicated improved thermal stability and lower moisture absorption compared to pure jute fiber composites. Morphological analysis using scanning electron microscopy revealed better fiber-matrix bonding, reduced fiber pull-out, and improved fracture behavior in the composites with higher banana fiber content. Majumder et. al.[19] focused on improving the thermal insulation properties of jute fiber-reinforced composite mortars. Jute fibers of varying lengths (5 mm, 10 mm, and 30 mm) and percentages (0.5%, 1%, 1.5%, and 2%) were added to the mortar to evaluate their effects. Results showed that as fiber percentage increased, thermal resistance improved, with longer fibers (30 mm) dissipating more mechanical energy and shorter fibers (5 mm) significantly reducing thermal conductivity, thereby enhancing insulation capacity. Zakriya et. al.[20] focused on the thermal properties of non-woven jute composite panels produced through compressive hot pressing, with jute fiber content ranging from 50%–70% and hollow conjugated polyester fiber from 30%–50%. The results indicated that composites with 3600 gsm (51/49 jute/polyester) at 5.0 mm thickness and 3200 gsm (76.5/23.5 jute/polyester) at 4.5 mm thickness showed optimal thermal responses. Duran[21] investigated the thermal insulation properties of single and double-layered needle-punched nonwovens produced using recycled jute and wool fibers, along with polyester and recycled wool. Results showed that recycled wool and wool fibers significantly improved the thermal insulation properties of the nonwoven structures. Additionally, recycled jute fibers were found to maintain thermal performance, making them suitable for insulation applications. Bhuiyan et al.[22] focused on the thermal properties of jute-reinforced polypropylene (jute-PP) biocomposites, exploring their potential for heat insulation in buildings. The developed composites exhibited low thermal conductivity and superior thermal barrier performance compared to commercial gypsum board. The composites also showed enhanced conductive and radiative heat resistance, making them ideal for insulation applications. Additionally, the presence of lignin in jute fiber contributed to comparable flame resistance, while low water absorption indicated good durability. Balan et. al.[23] investigated the fire resistance of woven jute fiber reinforced with fly ash, focusing on reducing flammability. Results showed that fly ash significantly reduced flammability. A composite with 5 wt% jute fiber, 15 wt% fly ash, and 10 hours of NaOH treatment achieved a minimum burning rate of 10.2 mm/min in horizontal UL-94 tests. Li et. al.[24] focused on enhancing the flame retardancy of jute fabric by treating it with a gel composed of chitosan (CH) and sodium alginate (SA). The gel was prepared through ion-ion interactions, with sodium chloride acting as a stabilizer. The treated jute fabric showed significant improvements in fire resistance, evidenced by a limiting oxygen index (LOI) of 27% and a reduced damaged length of less than 5 cm during vertical combustion testing. Additionally, the heat release capability of the treated fabric was reduced by 50%, showed a significant enhancement in flame retardancy compared to untreated jute fabric.

Despite the increasing interest in natural fiber composites, there remains a critical need to develop fire-retardant, thermally insulating, and mechanically robust structures that are also environmentally sustainable. While previous studies have explored mechanical, thermal, and flame-retardant improvements individually, there is limited research on

integrated sandwich structures combining these properties, especially using sodium silicate as a bonding agent with jute-based core and skin reinforcements. This research aims to address this gap by developing and evaluating hybrid jute/polyester fiber-based sandwich composites with varying sodium silicate concentrations.

In summary, previous studies have demonstrated the potential of jute fiber composites in improving mechanical, thermal, and fire-resistant properties through fiber treatment, hybridization, and structural design. However, the development of multifunctional, eco-friendly sandwich panels using recycled and natural materials remains an underexplored area. The present work builds on this foundation by introducing a novel sandwich configuration aimed at multifunctional performance for real-world applications.

In this work, novel sandwich structures were prepared using sodium silicate bonded non-woven hybrid jute/polyester fiber-based composites with different sodium silicate concentrations as core and a single layer woven jute fiber mat reinforced epoxy composite as skins. The aim is to develop sandwich structures that are lightweight, high load bearing capacity, thermally insulating, and fire-retardant for applications in ship/train cabin panels, building insulation, ceiling panels, etc. The physical, mechanical, thermal and fire behavior of the manufactured sandwich structures were investigated. The role of sodium silicate concentration on these properties were also explored.

Materials and methods

Materials

A non-woven mat as shown in Figure 1(a), consisting of 60% jute fiber and 40% polyester fiber of length 140-150 mm, was used to prepare the core of the sandwich structures. The jute mat was collected from Jute Textile Mills Ltd, Khulna, Bangladesh. The mat was characterized by its thickness and areal density. To determine the areal density, at first, the jute mat was cut into 25 mm by 25 mm sizes and their mass was recorded. The areal density of the jute mat was calculated as the ratio of its mass to the area. The average thickness and the areal density of the mat are 4.94 ± 0.06 mm and 0.080 ± 0.01 g/cm^2 respectively. Woven jute fiber mat as shown in Figure 1(b) also collected from the same company and was used for manufacturing the skins of the sandwich structure. The

Figure 1. (a) Non-woven hybrid jute/polyester mat and (b) woven jute mat.

thickness and areal density of the mat are 0.076 (±0.001) mm and 0.049 (±0.001) g/cm^2 respectively.

Sodium silicate solution (Na_2SiO_3) was collected from Silica solution, Chattogram, Bangladesh. Sodium silicate acts as a binder and fireproofing agent, suitable for applications where fire resistance is important, such as in construction, marine, automotive components.[25,26] Sodium silicate solution was used to manufacture non-woven hybrid jute/polyester fiber reinforced sodium silicate composite panels to be used as core of the sandwich structure. Sodium silicate solution has a solid content of 38.1% and SiO_2/Na_2O = 3.22.

Epoxy resin is a versatile, durable polymer, and when mixed with a hardener, it undergoes a chemical reaction to form a strong and rigid solid.[27] This resin-hardener combination is used to manufacture lightweight, high-strength composites in various industries like aerospace, automotive, and construction. It offers precise control over curing and exceptional bonding properties, making it a fundamental element in modern composite engineering.[28,29] Epoxy resin and a hardener of 2:1 from Lapox brand, country of origin India were collected and used to manufacture woven jute fiber reinforced epoxy composite to be used as skins of the sandwich structure. A pure epoxy sample was prepared to evaluate its properties. The density, strength, and elastic modulus of the pure epoxy sample was 1.11 (±0.01) g/cm^3, 38.63 (±4.17) MPa, and 2915.77 (±295.54) MPa respectively.

Sample preparation

In this work, non-woven hybrid jute/polyester fiber reinforced sodium silicate composites identified as "HSC", woven jute fiber reinforced epoxy composites identified as "JEC" and the sandwich structures using HSC as core and JEC as skins were prepared. The preparation processes of HSC, JEC, and sandwich are discussed below:

Preparation of HSC sample. The non-woven mat (60% jute & 40% polyester) was cut into a specific size (250 mm × 250 mm). Sodium silicate of 100% concentration (as received condition) was poured over the jute mat and distributed carefully using paint brush so that sodium silicate could wet all the fibers. Then the wetted jute mat was rolled 10 times using a flat roller to remove the excess sodium silicate. The wetted sample was initially dried at room temperature for 24 hours. Then it was placed in an oven (GALLENKAMP, UK) at 80°C until the weight stabilized. The weight of the sample was measured at every stage, and proper labeling of all samples was maintained. The same process was continued for sodium silicate concentrations of 90% (diluted with 10% distilled water) and 80% (diluted with 20% distilled water). The wet non-woven mat and the prepared HSC are shown in Figure 2(a) and (b) respectively.

Preparation of JEC. The epoxy resin and hardener were mixed at a ratio of 2:1 and mixed properly for at least 3 minutes. A plastic film was placed on top of a steel plate and the woven jute mat was placed on top of the film. The liquid epoxy mixture was poured on the jute fiber mat and distributed using a paint brush and a grooved plastic roller to remove

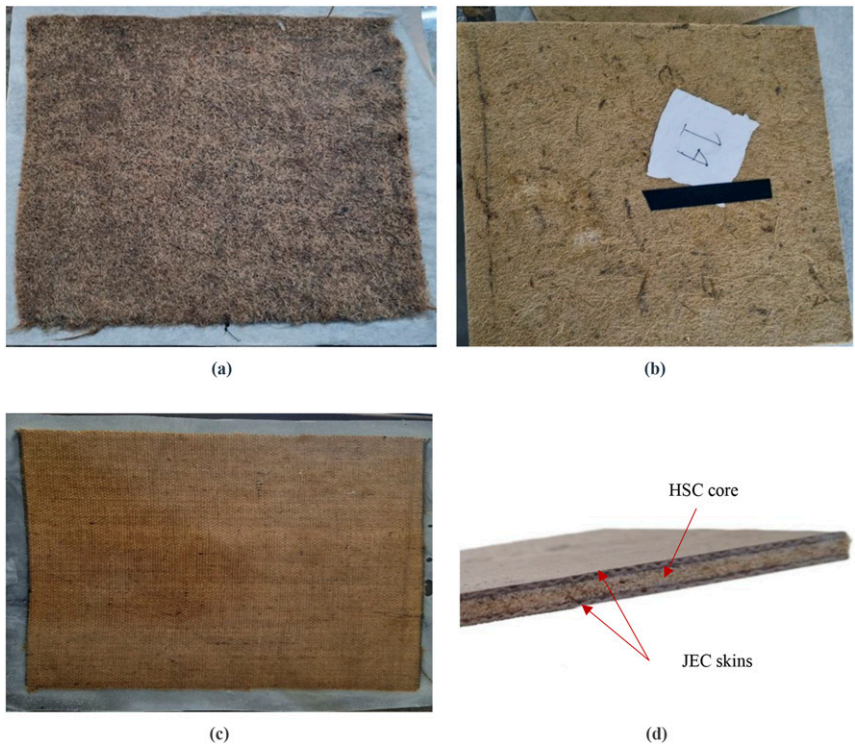

Figure 2. (a) Non-woven hybrid jute/polyester fiber after being wetted with sodium silicate solution, (b) dried HSC, (c) cured JEC, and (d) fabricated sandwich structure.

trapped air. Another plastic film was placed on top of the sample and remaining air bubbles were removed using a visiting card followed by another steel plate was placed on top of the plastic film and a load of 10 kg was placed on top of the top steel plate. The setup was kept for 48 hours for curing. The prepared JEC sheet is shown in Figure 2(c). The JEC sheet was tested in tension and the tensile strength and modulus were respectively 61.16 ± 7.50 MPa and 6.85 ± 1.82 GPa.

Sandwich fabrication. The sandwich composites were fabricated using HSC as core and JEC as skin by attaching JEC on both sides of HSC using the same epoxy resin adhesive used for manufacturing JEC. The adhesive layer uniformity was maintained. The sandwich structure was held between two steel plates and a load of 10 kg was placed on the top to ensure proper adhesion between the layers. The setup was kept at room temperature for 48 hours for curing according to the epoxy manufacturer's recommendation. The fabricated sandwich structure is shown Figure 3(d). For 80%, 90%, and 100% HSC-based sandwiches are identified as S80, S90, and S100 respectively.

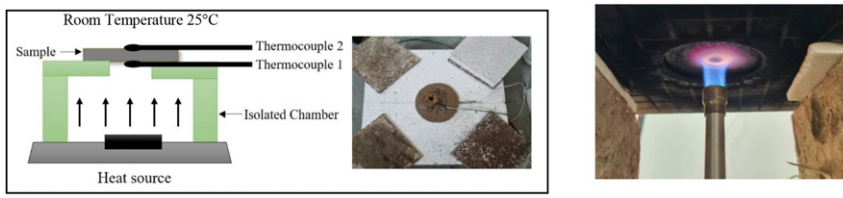

Figure 3. (a) Thermal and (b) fire exposure test setup.

Test methods

Density. For every sample, the length, width, and thickness were measured using digital slide calipers. The mass of the sample was measured using a weighing machine with precision of 0.001 g. The density of the sandwiches was calculated using the dimensions and the mass.

Mechanical test methods. The tension and flexural tests were conducted according ASTM D 3039 and ASTM D 738 standards respectively by using a universal testing machine (Shimadzu AGXV 300 kN, Japan) with a crosshead speed of 2 mm/min. The short beam strength test was conducted using the same machine according to ASTM D 2344 standard at a crosshead speed of 1 mm/min. The dimensions of the test specimens were 160 mm × 15 mm × t mm for tension test, 100 mm × 15 mm × t mm for flexural test, and 32 mm × 15 mm × t mm for short beam shear test.

Thermal exposure test. A test setup was developed for thermal exposure test as shown in Figure 3(a). The purpose of this test is to determine the temperature variation between the hot and cold side of the sample when the sample hot side temperature is approximately 71-73°C. The sample was positioned for testing with one side exposed to a regulated heat source as shown in Figure 3. The set temperature of the chamber was 70°C but the temperature was varied between 71 and 73°C. The temperature sensors (Pt100) were installed on both sides of the sample to measure the hot and cold side temperatures. The temperatures were recorded using a datalogger (Grpahtec). The air-conditioned test room temperature was maintained at 25°C. The test was carried out until both sides reached a steady-state condition.

Fire exposure test. The fire exposure test of the sandwich structures was conducted for qualitative evaluation of the fire resistance. The sandwich samples (S100, S90, and S80) were exposed to the flame produced using a Benson burner for 30 minutes as shown in Figure 3(b). The gas used to produce flame was liquified petroleum gas (LPG). A surface thermocouple (Pt100) was used at the center of the specimen on the unexposed surface of the sample to record the temperature rise. The unexposed surface temperature and the damage spread due to fire were observed to evaluate the fire performance.

Results and discussion

Mass of the constituents and density

The mass of the individual constituents per unit area in the HSC, JEC, and sandwich after manufacturing is given in Table 1. It is seen that the solid sodium silicate content in the core of the sandwich is decreased with decreased sodium silicate concentration during HSC manufacturing as expected.

Figure 4 shows the average density and standard deviation for the fabricated sandwich samples. The density decreased with the decrease in sodium silicate concentration as expected. The reason for this is that the skins were same for all sandwiches. Sample S100, which was manufactured using 100% of sodium silicate solution without any added water, has the highest average density of 0.82 g/cm^3. S90, with 90% of sodium silicate and 10% of water, has a slightly lower density of 0.78 g/cm^3, and S80, with the highest water content (20%), has the lowest average density at 0.73 g/cm^3 suggesting reduced solid sodium silicate content (see Table 1) in the core of the sandwiches.

Morphology

Figure 5(a) and (b) shows the cross-sectional view of chisel-cut surface of fabricated sandwich (S100). The cut surface shows a rough, textured core composed of non-woven jute fibers treated with sodium silicate. The core shows a highly heterogeneous structure, with fibers arranged in an irregular pattern as shown in Figure 5(b). In the core, the fibers have irregular orientation and distribution as expected due to randomly oriented fibers. The skin layers show a more uniform, dense surface compared to the core, indicating their role as protective outer layers in the composite sandwich structure. The interaction between the core and skin layers is visible at the interface and showing poor bonding between the skin and the core because of the uneven core surface due to excessively porous HSC. The sandwich core also reveals the excessive voids between the fibers of HSC. Figure 5(c) shows the sodium silicate coating on the surface of the fibers. It appears that the sodium silicate is highly compatible with the fiber and created good bonding.

Table 1. Mass of the individual constituent and the sandwich structure per unit area.

Sandwiches	Mass of woven mat, g/cm^2	Mass of the hybrid mat, g/cm^2	Solid sodium silicate in the HSC, g/cm^2	Mass of epoxy in JEC (g/cm^2)	Mass of epoxy in adhesive layer (g/cm^2)	Mass of epoxy in the sandwich (g/cm^2)
S100	0.049 (±0.001)	0.080 (±0.004)	0.076 (±0.016)	0.075 (±0.007)	0.042 (±0.015)	0.192 (±0.019)
S90			0.073 (±0.007)			
S80			0.052 (±0.016)			

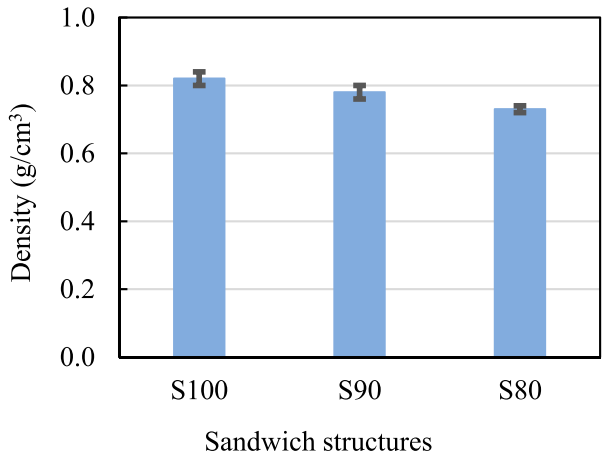

Figure 4. Density of sandwich structures.

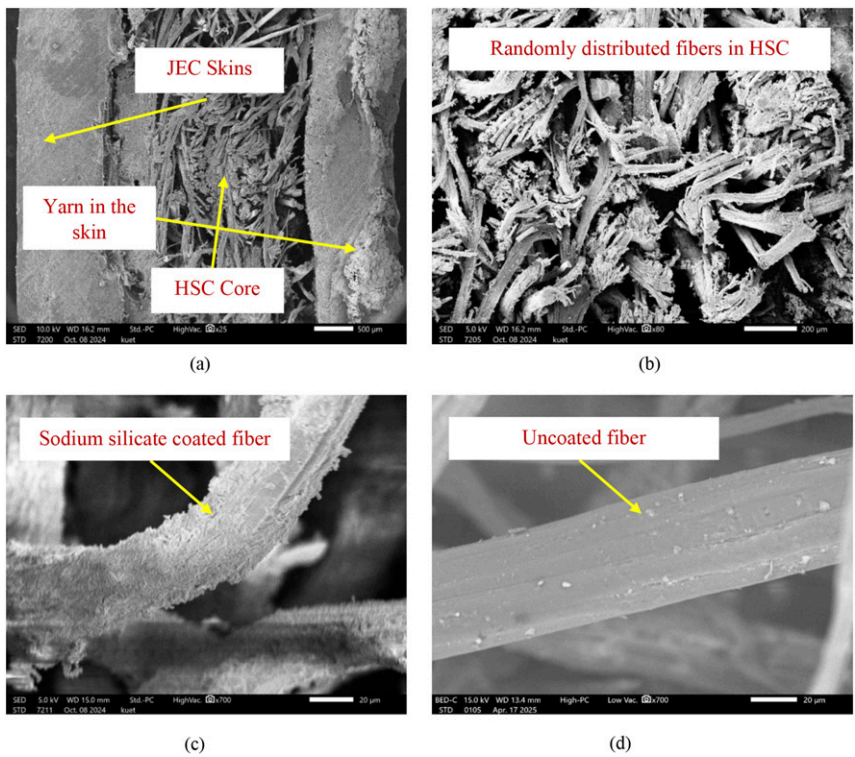

Figure 5. SEM of image of S100: (a) Chisel cut cross-section; (b) fracture surface; (c) sodium silicate coating and (d) uncoated fiber.

Mechanical properties

Tensile behavior. Figure 6 shows the stress-strain curves of different HSC cores and their sandwich structures. All samples showed a similar trend in the stress-strain curves, at first stress increased with strain linearly and reached at peak where failure took place suddenly except for C80 which showed gradual decline in stress after the instead of a sharp drop in stress. It is observed that the elongation at break is minimum for S100 and the maximum for S80 indicating that the higher sodium silicate concentration in the core causes early failure of the HSC cores and sandwiches. It is also found that the ultimate tensile stress and the slope of the stress-strain curve are maximum for S100 (C100 for HSC core) and for S80 (C80 for HSC core) and S90 (C90 for HSC core), they are lower than S100 (C100 for HSC core). It suggests that the increase in sodium silicate concentration increases the ultimate stress and modulus of the HSC cores and sandwiches. The stress-strain curve analysis shows that sodium silicate treatment improved the interfacial bonding between the hybrid fibers in the HSC, resulting in enhanced tensile strength and modulus of both HSC cores and sandwiches. During the tension test of sandwiches, it is observed that the failure first occurs in the sandwich core before reaching the peak stress for both S90 and S80 but for S100, the failure was not noticed until the peak strength. Some photographs of the failed specimens are given in Figure 7. The premature failure of the sandwich core for S90 and S80 can be related to the significant drop in the slope of the stress-strain curves of those sandwiches after the initial linear portion.

The tensile properties of the sandwiches and HSC cores are given in Table 2. The tensile strength for S100, S90, S80, C100, C90, and C80 are 23.51 MPa, 20.18 MPa, 20.48 MPa, 5.21 MPa, 4.75 MPa, and 3.51 MPa respectively. The tensile strength and tensile modulus of different samples are also shown in Figure 8 with standard deviation indicated by error bars.

The maximum tensile strength and tensile modulus for HSC core were found in C100 containing the undiluted sodium silicate solution. Diluting the sodium silicate solution for manufacturing HSC core results in decreased tensile strength and modulus as shown in Table 2 and Figure 8. Adding 20% water for diluting sodium silicate solution

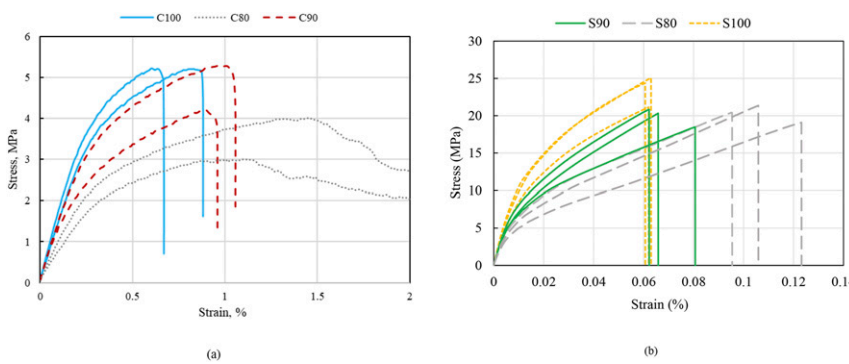

Figure 6. Some typical tensile stress-strain curves for (a) HSC cores and (b) sandwiches.

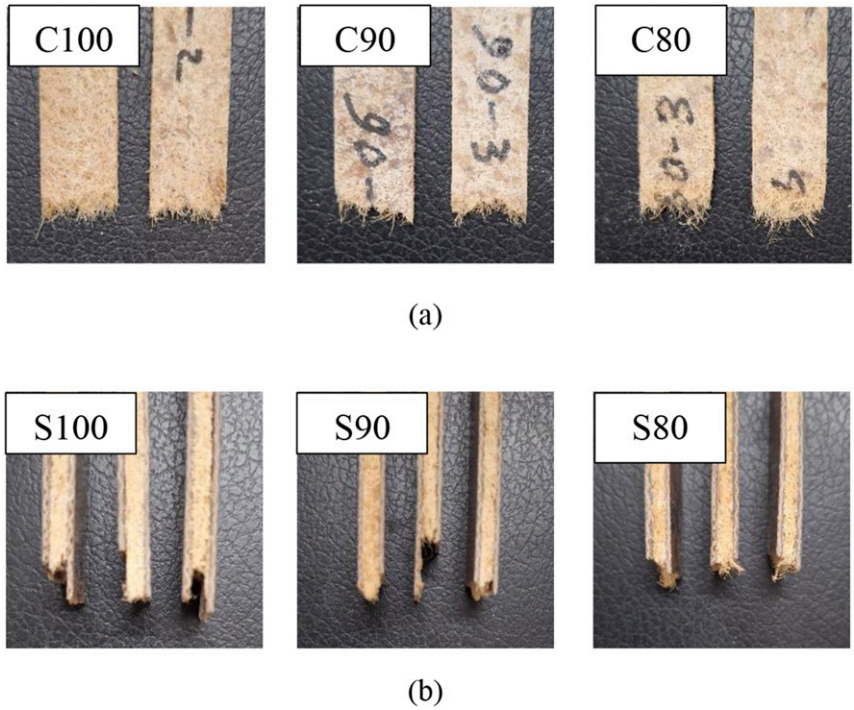

Figure 7. Typical failed specimen after tension test for (a) HSC cores and (b) sandwiches.

Table 2. Tensile properties of different sandwiches and their cores.

Sandwiches	Tensile strength (MPa)	Tensile modulus (MPa)	HSC core	Tensile strength (MPa)	Tensile modulus (MPa)
S100	23.51 (±1.13)	1281.03 (±111.35)	C100	5.21 (±0.01)	1642.10 (±309.18)
S90	20.18 (2.13)	1130.98 (±40.87)	C90	4.75 (±0.77)	1550.72 (±396.23)
S80	20.48 (±0.78)	959.05 (±65.28)	C80	3.51 (±0.71)	886.85 (±254.64)

(C80) decreased the tensile strength and modulus by 32.63% and 45.99% respectively. It is expected that a higher sodium silicate content in the would result in increased tensile properties because of a better bonding between the fibers.

The maximum tensile strength was seen in S100 sandwich. The tensile strength was decreased by 14.16% for S90 and 12.89% for S80 compared to S100. Approximately similar tensile strength was noticed for S90 and S80. All three types of sandwiches have similar skins and the skins tensile load bearing capacity is significantly higher than the HSC cores with small amount of sodium silicate as binder. Therefore, the skins are mostly responsible for the development of the tensile strength of the sandwiches and the

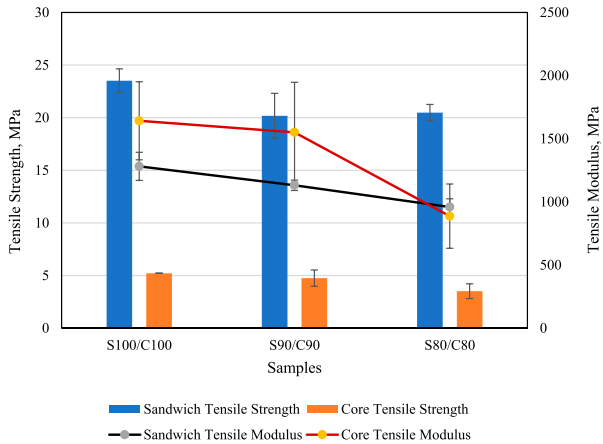

Figure 8. Tensile strength and modulus of different samples.

contribution of core is minimal because of the premature failure of the core specifically for S90 and S80. S100 sandwich has the maximum solid sodium silicate content as shown in Table 1 and the premature failure of the core of this sandwich was not noticed during tensile test. The reason for relatively higher tensile strength of S100 compared to S90 and S80 is mainly the contribution of the higher sodium silicate content in the core that prevented the premature failure of the core to some extend until the peak strength. Besides the C100 core also showed higher tensile strength as shown in Table 2. For S90 and S80, although sodium silicate is present in the core but due to high load-bearing capacity of the JEC skins compared to the core and the premature failure of the core before reaching the peak strength, their contribution was not reflected. These are the reasons for almost similar tensile strength of S90 and S80.

The slope of the initial linear portion of the tensile stress-strain curve was taken as the tensile modulus of the sandwiches and given in Table 2 as well as in Figure 8. The tensile modulus for S100, S90, and S80 sandwiches were found to be 1281.03 MPa, 1130.98 MPa and 959.05 MPa respectively. It is observed that the tensile modulus decreased consistently with the decrease in sodium silicate content in the core of the sandwiches. The tensile modulus was decreased by 11.71% for S90 and by 25.13% for S80 compared to S100. The effect of premature failure was not reflected in the tensile modulus of S90 and S80 sandwiches because the initial linear portion of the stress-strain curves were taken as the tensile modulus of the sandwiches. Therefore, the solid sodium silicate content in the core has significant contribution on the tensile modulus of the sandwiches that is, the higher the sodium silicate content in the core higher the tensile modulus. The tensile strengths of the sandwiches are significantly higher than the HSC cores but the tensile modulus of the sandwiches are lower than the HSC cores as shown in Figure 8. The rule of mixture may be used to predict the tensile modulus of the sandwiches. The equation for the rule of mixture may be written as:

$$\text{The tensile modulus of the sandwich, } E_{eff} = \left(E_f t_f + E_c t_c\right)/t_s \quad (1)$$

where, E_f, E_c, t_f, t_c, and t_s are elastic modulus of JEC skin, elastic modulus of the HSC core, thickness of JEC skin, thickness of HSC core, and thickness of the sandwich respectively.

The average skin thickness for all composites is 1.13 ± 0.08 mm and average core thicknesses for S100, S90 and S80 are respectively 3.34 ± 0.30 mm, 3.15 ± 0.25 mm, 3.42 ± 0.42 mm. The tensile moduli of HSC cores are 1642.10 MPa for C100, 1550.72 for C90, and 886.85 MPa for C80. The tensile modulus of JEC skin is 6850 MPa. Considering a thin adhesive layer and according to the equation (1) the elastic modulus for the sandwiches was estimated and shown in Table 3.

From Table 3 it is seen that the measured tensile moduli of the sandwich composites were significantly lower than the predicted values based on the rule of mixtures. This difference suggests ineffective load transfer between the skin and core, due to poor interfacial bonding as discussed in Section "Morphology" or local debonding or slippage during tensile loading. This behavior is consistent with literature,[30] where poor skin–core adhesion significantly reduces the effective stiffness despite high skin modulus. It is also possible that defects, such as voids or adhesive-rich zones at the interface, contributed to early strain localization and reduced stiffness response.

Flexural behavior. The typical graphs, shown in Figure 9, illustrates the variation in stress with strain for different HSC cores and sandwiches during flexural tests. For HSC cores, the stress increases linearly with respect to strain up to a peak and gradually drops. For sandwiches, initially stress increased linearly with strain up to a peak where crack in the core was observed. For sandwiches, the stress also increases linearly with strain up to a peak and after that the stress gradually decreased to some extend followed by an upward trend (for some samples) to a second peak (the second peak is lower than the first one). A further increment in the strain, the stress decreased gradually until skin delamination takes place which is reflected by the sudden drop and plateau in stress in the stress-strain curves as shown in Figure 9(b). The failure at the first peak is mainly due to the core shear cracking. After the first peak the load is primarily carried by the skins of the sandwich structure. The gradual increase after failure and plateau in the stress-strain curves. Eventually multiple cracks and delamination were noticed in the core of the sandwich structures as the displacement continued. The failure in the HSC core is mainly due to cracking at the bottom side of the sample and for sandwiches the failure is mainly core

Table 3. Predicted and measured elastic modulus of the sandwiches.

Sandwiches	HSC core modulus (MPa)	Predicted sandwich modulus (MPa)	Measured sandwich modulus (MPa)
S100	1642.10	3744.6	1281.03
S90	1550.72	3763.5	1130.98
S80	886.85	3259.7	959.05

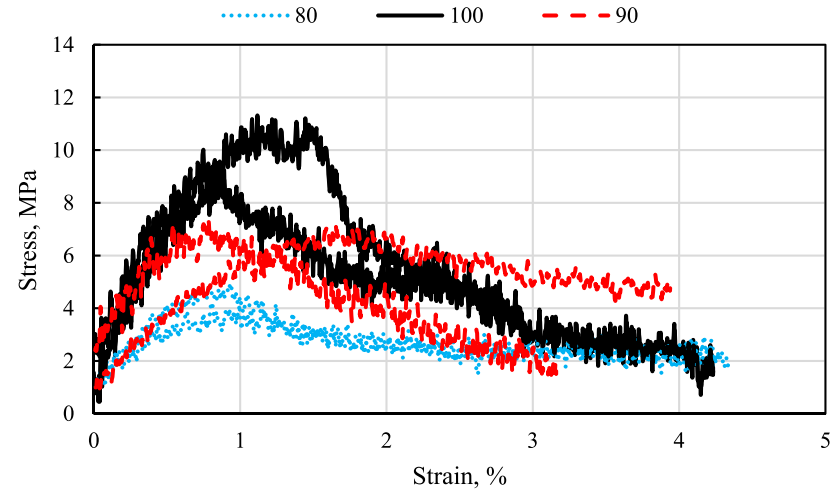

(a)

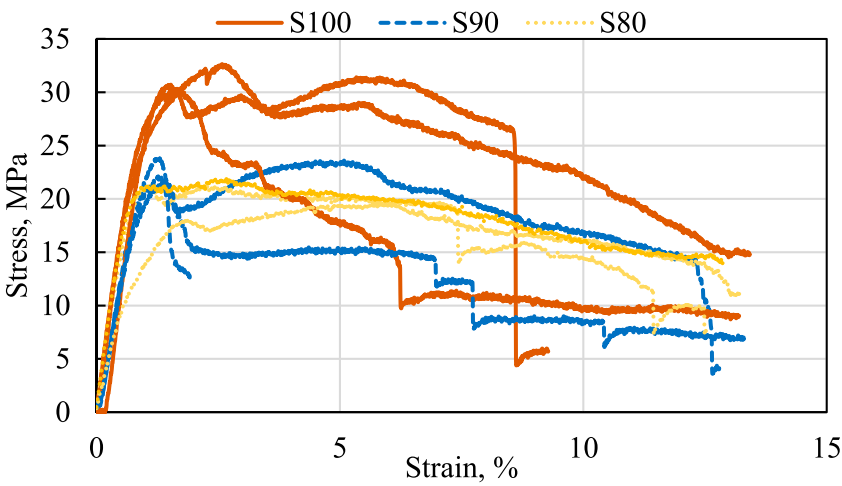

(b)

Figure 9. Typical flexural stress-strain curves for (a) HSC cores and (b) sandwiches.

shear cracking followed by skin delamination. The failed samples for HSC cores and sandwiches are shown in Figure 10.

The flexural strength and modulus of the HSC cores and sandwiches are given in Table 4 and plotted in Figure 11 with standard deviations as error bars.

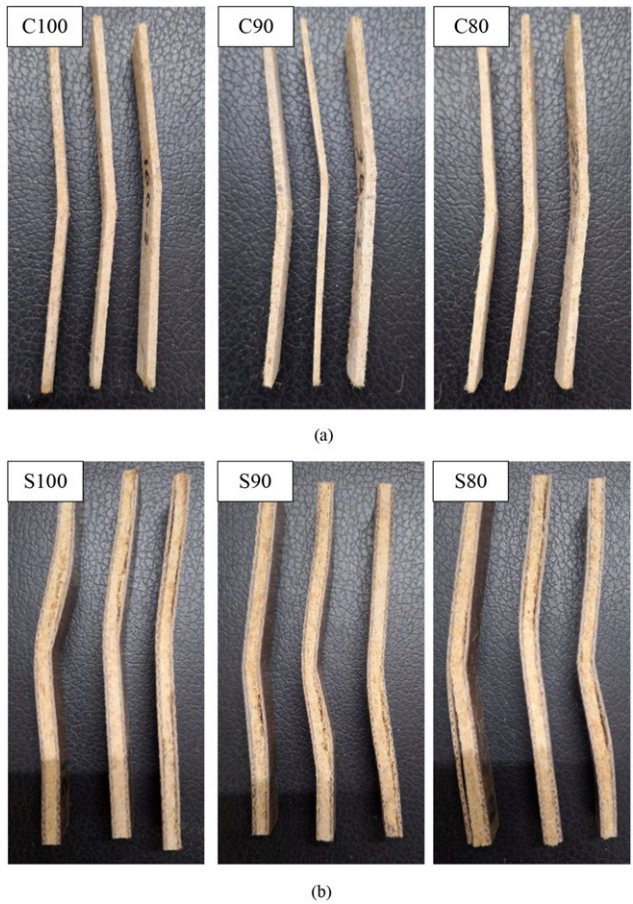

Figure 10. Flexural test sample after test: (a) HSC cores and (b) sandwiches.

Table 4. Flexural properties of different sandwiches and their cores.

Sandwiches	Flexural strength (MPa)	Flexural modulus (MPa)	HSC core	Flexural strength (MPa)	Flexural modulus (MPa)
S100	31.58 (±1.24)	3460.15 (±247.40)	C100	11.11 (±2.39)	1203.79 (±175.51)
S90	22.52 (±1.15)	2586.53 (±283.61)	C90	7.93 (±0.09)	698.90 (±291.90)
S80	21.05 (±1.06)	1985.73 (±772.85)	C80	5.38 (±0.62)	464.20 (±92.43)

The flexural strength of C100, C90, and C80 are 11.11 MPa, 7.93 MPa, 5.38 MPa respectively. As expected, the flexural strength of HSC cores decreased with increased dilution of sodium silicate solution. The decreased sodium silicate content for C90 and C80 causes weak bonding between the fibers resulting a lower strength. The flexural

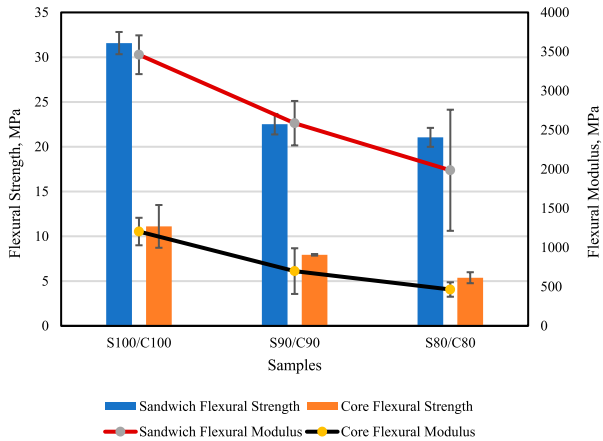

Figure 11. Flexural strength and modulus of different samples.

modulus of HSC cores also showed similar behavior for example, lower the sodium silicate content lower the modulus as shown in Table 4 and Figure 11.

The flexural strength of S100, S90, and S80 are 31.58 MPa, 22.52 MPa, and 21.05 MPa respectively. It is seen that the S100 exhibited the maximum flexural strength compared to both S90 and S80. The flexural strength of S90 and S80 were respectively 28.68% and 33.33% lower than that for S100. Since the concentration of solid sodium silicate in the core of S100 is maximum as shown in Tables 1, it can be said that the flexural strength decreases with a decrease in the concentration of sodium silicate in the core. The reason for lower flexural strength of S90 and S80 is that the smaller amount of solid sodium silicate could not provide sufficient bonding between the fibers for resisting shear cracking during flexural test resulting in a lower peak stress.

The flexural modulus of S100 is found to be the maximum as expected due to high sodium silicate content in the core of the sandwich. The flexural modulus dropped gradually for S90 and S80. Although the flexural strength of S90 and S80 is almost similar but the flexural modulus of S80 is significantly lower than S90. Note that the flexural strength is related to the peak load in the load-displacement curves but the flexural modulus is related to the slope of the initial linear portion of the stress-strain curve. Due to high sodium silicate content in the core for S100 the load bearing capacity of the core is high and the slope of the initial linear portion of the stress-strain curve is also high. The sandwiching of HSC cores with JEC skins significantly increased the flexural strength and modulus.

Short beam strength

Figure 12 shows the short beam shear strength of the fabricated sandwiches. During testing, it was observed that the failure initiation for all samples was in the core of the sandwich suggesting an efficient bonding between the core and the sandwiches. However,

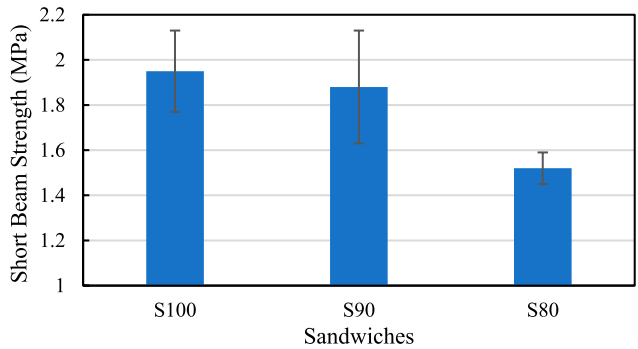

Figure 12. Short beam strength of different sandwiches.

in some cases, the core cracking was followed by the skin delamination due to further displacement of the loading roller. After calculation, S100 and S90 showed almost similar short beam strength but the strength decreased in the case of S80 samples. Since the short beam strength is related to the peak force at which the shear failure takes place during bending test, it can be hypothesis that the higher shear strength of the core and proper bonding between the skin and the core would result in a high short beam strength. Since the failure initiation was in the core by shear cracking, the reason for a higher short beam strength of S100 and S90 compared to S80 is the proper bonding of the fibers in the core due to high sodium silicate content.

Thermal exposure test results

In the thermal exposure test, the inside chamber temperature was maintained around 71 °C–73°C. The outside temperature of the sample was measured for S100, S90 and S80 samples which are 43.61°C, 44.11°C and 44.68°C respectively as shown in Figure 13. The effect of sodium silicate content of HSC core on the heat transfer capabilities of the composites appeared to be insignificant according to the results of the thermal exposure test conducted on the three composite samples. Considering convective heat transfer coefficient of air as 10 W/m^{2}K, the thermal conductivity of the sandwiches may be calculated using the equations below:

$$\text{Heat flux}, q = h(T_o - T_\infty) \tag{2}$$

$$\textit{Thermal conductivity}, k = q.d/(T_i - T_o) \tag{3}$$

where, h, d, T_i, T_o, T_∞ are convective heat transfer coefficient of air, thickness of sandwich, inside surface temperature of the sandwich, outside surface temperature of sandwich, ambient temperature of the room respectively.

Although this may not provide the accurate thermal conductivity of the sandwiches but would provide an understanding on the heat insulation capability of the sandwiches. The

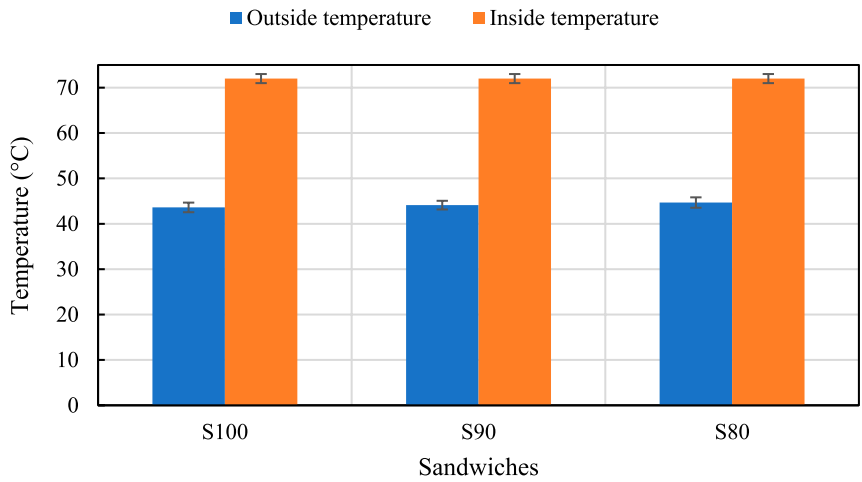

Figure 13. Comparison of outside and inside temperature of different sandwiches during thermal exposure test.

thermal conductivity of the S100, S90, and S80 was found to be respectively, 0.037 W/mK, 0.036 W/mK, and 0.041 W/mK. It was expected that the sodium silicate coating would significantly increase the thermal conductivity of the sandwiches due to its relatively high thermal conductivity. However, it appears that the thermal conductivity of sandwiches was not significantly affected by the sodium silicate coating because the excessively porous structure of the cores as seen in Figure 5(b). The thermal conductivities of the sandwiches are close to the thermal conductivity of air and are lower than many existing composites in the literature. For instance, Bhuiyan et al.[31] evaluated the thermal conductivity of jute-reinforced composites as 0.2694 W/m.K for jute in polyethylene and 0.1852 W/m.K for jute in polypropylene. Jawaid et al.[32] determined thermal conductivity of pure epoxy, pure jute/epoxy, pure empty fruit branch (EFB)/epoxy, and hybrid fiber epoxy composites and obtain thermal conductivity ranges from 0.2471 to 0.2976 W/m·K. Pujari et al.[33] also evaluated the thermal conductivity of pure jute epoxy composite which is 0.23 W/m·K. It can be seen that the thermal conductivity of the developed composite sandwich structures is significantly lower than some of the existing jute based composite materials. Therefore, these sandwich composites may be useful for insulation.

Fire exposure test

In the fire exposure test, after 30 minutes of burning the temperature of the unexposed surface are given in Figure 14. It is seen that the maximum unexposed surface temperature was found for the S80 and the lowest was found for the S100 sandwich. The unexposed surface temperature of S80 showed approximately 30°C higher then S100 indicating the effectiveness of sodium silicate treatment of the core of the sandwiches. The photographs

of the damaged sandwiches after 30 minutes of exposure are given in Figure 15. It can be seen that the damage spread on the fire exposed and unexposed surfaces (see Figure 15) is maximum for S80 and minimum for S100 indicating the effectiveness of high sodium silicate content in the core. The severe damage can be seen on the unexposed surface of the S80 sandwich whereas the S100 sandwich show the minimum affected area as shown

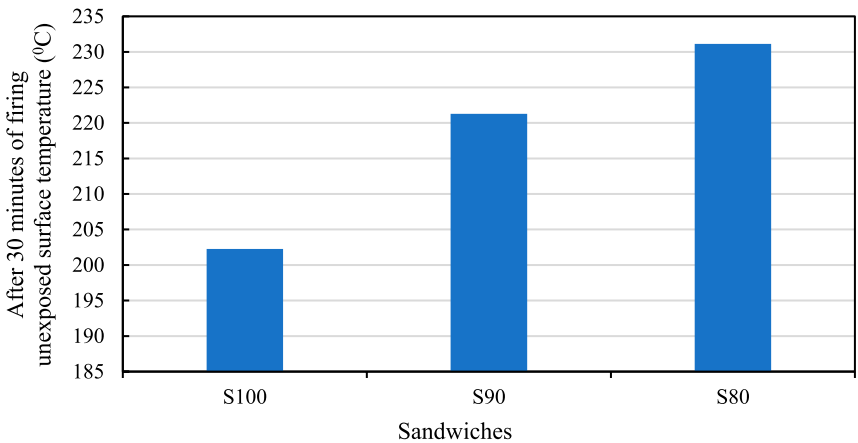

Figure 14. Comparison of unexposed surface temperature of different sandwiches after 30 minutes of burning.

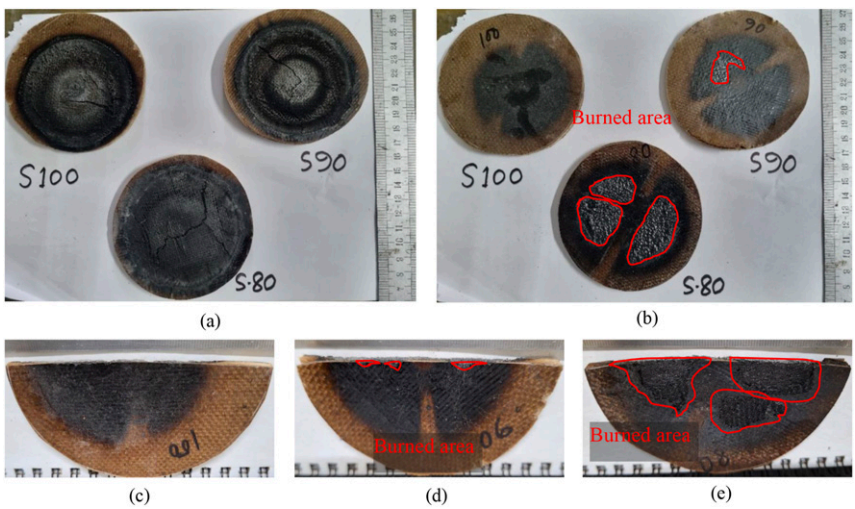

Figure 15. Photographs of the sandwiches after fire exposure test (a) exposed surface, (b) unexposed surface, and (c)-(e) unexposed surface cut through the center.

in Figure 15(c)-(e). These observations suggest that S100 sandwich shows better fire resistance compare to other two because of the high solid sodium silicate content in the HSC core of the sandwich.

Using ImageJ and Figure 15(b) the affected area on the unexposed surface was calculated and it is seen that the affected area for S90 and S80 are approximately 2.21 cm^2 and 22.29 cm^2 respectively. For S100, the unexposed skin damage was not noticed. Above observation provides a good insight on the effectiveness of sodium silicate treated core on protecting fire damage of the sandwich structure. The is investigation paves the way for further investigation on utilizing fire resistant core for sandwich structures.

Conclusions

The novel lightweight sandwich structures were fabricated using sodium silicate bonded non-woven jute and polyester hybrid fiber-based core and woven jute fiber reinforced epoxy composite as skins. The effect of sodium silicate concentration on the tensile, flexural, thermal, and fire behavior of sandwich structures were investigated. The findings are summarized below:

- The tensile and flexural properties of the sandwiches are significantly affected by the sodium silicate concentration in the core of the sandwich structure. A higher sodium silicate concentration in the core leads to a higher the strength and modulus of the sandwiches but the density of the sandwiches increased. The flexural strength of S100 is respectively 28.68% and 33.33% greater than S90 and S80 sandwiches.
- The thermal conductivity of sandwiches is not significantly affected by the dilution of the sodium silicate solution for preparing the core of the sandwiches. The thermal conductivity of the developed sandwiches (0.036 W/mK-0.041 W/mK) is found to be lower than many available jute-based composites in the literature.
- The sodium silicate concentration plays a significant role on fire resistance of the sandwiches. The sandwich made of a core with high sodium silicate content reduces the heat flow towards the unexposed surface of the sandwich. The unexposed surface temperature of S100 is found to be approximately 30°C less than S80 sandwich for 30 minutes of fire exposure.
- A high sodium silicate content in the core of the sandwich structure also helped reducing the fire spread on the exposed surface and damage propagation towards the unexposed surface of the sandwich. The affected unexposed surface area for S90 and S80 are approximately 2.21 cm^2 and 22.29 cm^2 respectively whereas for S100 the unexposed surface was not affected due to fire exposure for 30 minutes.
- The novel sandwiches reported in this work may be suitable for applications which require high strength, insulation, and fire resistance simultaneously. Improving the bonding between the core and the skin may improve the mechanical properties of the sandwiches further.

- Although this work demonstrates the effectiveness of sodium silicate treated hybrid jute/polyester fiber core on the mechanical, thermal and fire behavior of the sandwich structures, further research is necessary because of the variations in hybrid fiber mat (e.g., thickness, fiber distribution, etc.) in different batches.

Declaration of conflicting interests

The author(s) declared no potential conflicts of interest with respect to the research, authorship, and/or publication of this article.

Funding

The author(s) disclosed receipt of the following financial support for the research, authorship, and/or publication of this article: The authors acknowledge Khulna University of Engineering & Technology for providing the partial funding for this work.

ORCID iDs

Md Arifuzzaman https://orcid.org/0000-0003-3657-5650
Md Shariful Islam https://orcid.org/0000-0003-3591-3793

References

1. Bhong M, Khan TK, Devade K, et al. Review of composite materials and applications. *Mater Today Proc* 2023. doi:10.1016/j.matpr.2023.10.026.
2. Vijay N, Rajkumara V and Bhattacharjee P. Assessment of composite waste disposal in aerospace industries. *Procedia Environ Sci* 2016; 35: 563–570.
3. Chandramohan D, Sathish T, Dinesh Kumar S, et al. Mechanical and thermal properties of jute/aloevera hybrid natural fiber reinforced composites. In: *AIP Conference Proceedings*. New York: AIP Publishing, 2020.
4. Naik V, Kumar M and Kaup V. A review on natural fiber composite material in automotive applications. *Eng Sci* 2021; 18: 1–10.
5. Khatri H, Dua S, Naveen J, et al. Potential of natural fiber based polymeric composites for cleaner automotive component production-a comprehensive review. *Journal of Materials Research and Technology* 2023; 25: 1086–1104.
6. Shakir MH and Singh AK. Mechanical properties, surface treatments, and applications of jute fiber reinforced composites—a review. *Polym Adv Technol* 2024; 35(1): e6268.
7. Etale A, Onyianta AJ, Turner SR, et al. Cellulose: a review of water interactions, applications in composites, and water treatment. *Chem Rev* 2023; 123(5): 2016–2048.
8. Verma A, Jain N and Mishra RR. Applications and drawbacks of epoxy/natural fiber composites. In: *Handbook of epoxy/fiber composites*. Berlin: Springer, 2022, pp. 1–15.
9. Kumar TS, Kumar SS and Kumar LR. Jute fibers, their composites and applications. In: *Plant fibers, their composites, and applications*. Amsterdam: Elsevier, 2022, pp. 253–282.
10. Kabir MM, Islam MM and Wang H. Mechanical and thermal properties of jute fibre reinforced composites. *Journal of Multifunctional Composites* 2013; 1(1): 71–76.

11. Bisaria H, Gupta M, Shandilya P, et al. Effect of fibre length on mechanical properties of randomly oriented short jute fibre reinforced epoxy composite. *Mater Today Proc* 2015; 2(4-5): 1193–1199.
12. Wang F, Lu M, Zhou S, et al. Effect of fiber surface modification on the interfacial adhesion and thermo-mechanical performance of unidirectional epoxy-based composites reinforced with bamboo fibers. *Molecules* 2019; 24(15): 2682.
13. Rajole S, Ravishankar K and Kulkarni S. Performance study of jute-epoxy composites/ sandwiches under normal ballistic impact. *Def Technol* 2020; 16(4): 947–955.
14. Elbadry EA, Aly-Hassan MS and Hamada H. Mechanical properties of natural jute fabric/jute mat fiber reinforced polymer matrix hybrid composites. *Adv Mech Eng* 2012; 4: 354547.
15. Fajrin J, Zhuge Y, Bullen F, et al. Flexural behaviour of hybrid sandwich panel with natural fiber composites as the intermediate layer. *J Mech Eng Sci* 2016; 10(2): 1968–1983.
16. Manfredi LB, Rodríguez E, Wladyka-Przybylak M, et al. Thermal properties and fire resistance of jute-reinforced composites. *Compos Interfaces* 2010; 17(5-7): 663–675.
17. Singh AA. Thermal properties of jute fiber reinforced chemically functionalized high density polyethylene (JF/CFHDPE) composites developed by palsule process. *Polym Compos* 2014; 2(2): 97–108.
18. Boopalan M, Niranjanaa M and Umapathy M. Study on the mechanical properties and thermal properties of jute and banana fiber reinforced epoxy hybrid composites. *Compos B Eng* 2013; 51: 54–57.
19. Majumder A, Stochino F, Frattolillo A, et al. Jute fiber-reinforced mortars: mechanical response and thermal performance. *J Build Eng* 2023; 66: 105888.
20. Zakriya GM, Ramakrishnan G, Palani Rajan T, et al. Study of thermal properties of jute and hollow conjugated polyester fibre reinforced non-woven composite. *J Ind Textil* 2017; 46(6): 1393–1411.
21. Duran D. A research on thermal insulation properties of nonwovens produced with recycled jute and wool fibres. *Textile and Apparel* 2016; 26(1): 22–30.
22. Bhuiyan MAR, Ali A, Akter H, et al. Flame resistance and heat barrier performance of sustainable plain-woven jute composite panels for thermal insulation in buildings. *Appl Energy* 2023; 345: 121317.
23. Balan GS, Balasundaram R, Chellamuthu K, et al. Flame resistance characteristics of woven jute fiber reinforced fly ash filled polymer composite. *J Nanomater* 2022; 2022(1): 9704980.
24. Li S-Q, Tang R-C and Yu C-B. Flame retardant treatment of jute fabric with chitosan and sodium alginate. *Polym Degrad Stabil* 2022; 196: 109826.
25. Sankar K, Stynoski P, Al-Chaar GK, et al. Sodium silicate activated slag-fly ash binders: Part I–Processing, microstructure, and mechanical properties. *J Am Ceram Soc* 2018; 101(6): 2228–2244.
26. Chen S-N, Li PK, Hsieh TH, et al. Enhancements on flame resistance by inorganic silicate-based intumescent coating materials. *Materials* 2021; 14(21): 6628.
27. Saba N and Jawaid M. Epoxy resin based hybrid polymer composites. *Hybrid polymer composite materials* 2017; 2017: 57–82.
28. Al Mahmud MZ, Chowdhury MS, Rayhan MT, et al. Epoxy resin composites reinforced with upcycled fabrics: mechanical, thermal, and morphological analysis. *SPE Polymers* 2024; 5(4): 624–636.

29. Ahammad R, Arifuzzaman M and Islam MS. Effect of micro-perlite powder content on thermo-mechanical properties of epoxy resin. *Polym Compos* 2025; 34: 09540083221092147.
30. Marx J and Rabiei A. Tensile properties of composite metal foam and composite metal foam core sandwich panels. *J Sandw Struct Mater* 2021; 23(8): 3773–3793.
31. Bhuiyan MAR, Darda MA, Ali A, et al. Heat insulating jute-reinforced recycled polyethylene and polypropylene bio-composites for energy conservation in buildings. *Mater Today Commun* 2023; 37: 106948.
32. Jawaid M, Saba N, Alothman OY, et al. Thermal conductivity behavior of oil palm/jute fibre-reinforced hybrid composites. In: *AIP conference proceedings*. New York: AIP Publishing, 2017.
33. Pujari S, Ramakrishna A and Balaram Padal KT. Investigations on thermal conductivities of jute and banana fiber reinforced epoxy composites. *J Inst Eng India Ser D* 2017; 98: 79–83.